Structural Engineering and Mechanics, *Vol. 56, No. 6 (2015) 983-1001*
DOI: http://dx.doi.org/10.12989/sem.2015.56.6.983

Shear behavior of multi-hole perfobond connectors in steel-concrete structure

Xing Wei*[1], Lin Xiao[1a] and Shiling Pei[2b]

[1]*School of Civil Engineering, Southwest Jiaotong University, Chengdu, China*
[2]*Department of Civil and Environmental Engineering, Colorado School of Mines, Golden, USA*

(Received January 27, 2015, Revised November 16, 2015, Accepted November 24, 2015)

Abstract. This study focuses on the load carrying capacity and the force transfer mechanism of multi-hole perfobond shear connectors in steel-concrete composite structure. The behavior of multi-hole perfobond shear connector is more complicated than single-hole connector cases. 2 groups push-out tests were conducted. Based on the test results, behavior of the connection was analyzed and the failure mechanism was identified. Simplified iterative method and analytic solution were proposed based on force equilibrium for analyzing multi-hole perfobond shear connector performance. Finally, the sensitivity of design parameters of multi-hole perfobond shear connector was investigated. The results of this research showed that shear force distribution curve of multi-hole perfobond shear connector is near catenary. Shear forces distribution were determined by stiffness ratio of steel to concrete member, stiffness ratio of shear connector to steel member, and number of row. Efficiency coefficient was proposed to should be taking into account in different limit state.

Keywords: steel-concrete composite structure; perfobond shear connectors; push-out tests; mechanical behavior; simplified calculation

1. Introduction

In typical steel-concrete composite structural members, the force transfer between concrete and steel is often ensured by dowel-type shear connectors. The behavior of the shear connection will influence the global behavior of the structural system. The behavior of specific shear connector configuration details has been a focus for composite structure research in the past. Although it can be categorized as a shear connector, the concept of perfobond shear connectors is relatively new and has not been fully understood. As it is shown in Fig. 1, Perfobond shear connectors are made of a steel plate with a number of uniformly spaced holes. When the holes in perfobond rib are filled with concrete, concrete dowels are formed. Longitudinal shear resistance of perfobond rib shear connector is provided by concrete end-bearing resistance, concrete dowel action, and transverse rebars in the rib holes. Steel perfobond rib shear connectors were first developed by

*Corresponding author, Associated Professor, E-mail: we_star@swjtu.cn
[a]Assistant Professor, E-mail: xiaolin@home.swjtu.edu.cn
[b]Assistant Professor, E-mail: spei@mines.edu

http://www.techno-press.org/?journal=sem&subpage=8 ISSN: 1225-4568 (Print), 1598-6217 (Online)

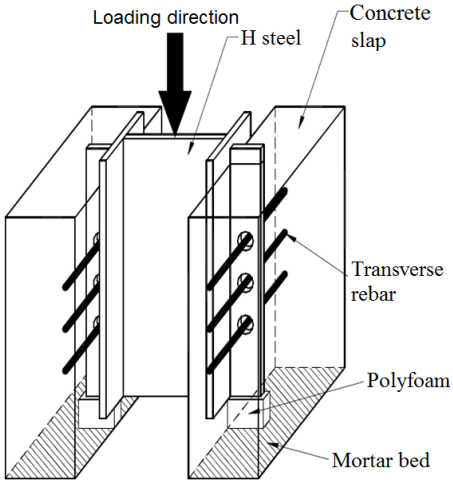

Fig. 1 Typical perfobond connection example

Zellner (1987) to address the problem of fatigue occurring in the stud shear connectors induced by live loads in railway bridges. Perfobond connector was firstly used in steel-concrete composite action between the steel I-girder and concrete deck by Leonhardt *et al.* (1987).

Quite a number of researchers have investigated behavior of perfobond connections through experimental and analytical methods. Veldanda and Hosain (1992) conducted push-out tests to check the applicability of the perfobond connector to composite floor systems. Different formulas were proposed by researchers for perfobond rib connectors based on numerous tests and finite element analyses. (e.g., Oguejiofor and Hosain 1997, Medberry and Shahrooz 2002, Chung and Lee 2005, Vianna *et al*. 2013, 2009). Modified shear-capacity equations that consider the perfobond rib arrangement, including rib height and spacing, are proposed by Ahn *et al*. (2010); The behaviors of steel-concrete composite slabs under bending with perfobond shear connectors were investigated by Kim and Jeong (2006). Rodrigues and Laím (2011) carried out tests focus on the behavior of perfobond shear connectors at high temperature condition. Advanced modeling methods, such as BP neural network analysis, were used to predict shear resistance of perfobond shear connectors in steel-concrete composite structure (Wei and Xiao 2011). Based on test result, ductility, stress distribution and collapse modes of perfobond rib connectors were studied. (e.g., Costa-Neves *et al.* 2013, Cândido-Martins *et al.* 2010, Wei and Xiao 2013). The behavior of composite girder with Y-type perfobond rib shear connectors were investigated by Kim *et al.* (2013, 2014, 2015). The behavior of steel-concrete composite decks with perfobond shear connectors was investigated by Hamed *et al.* (2014).

Compared with single-hole perfobond connection, the behavior of multi-hole perfobond connection is quite complicated. To date, a simplified approach has been taken in practice engineering calculation that the capacity of a multi-hole perfobond connection can be calculated by multiplying the single perfobond connector capacity by the number of connectors. However, this may not be true as the perfobond connector behavior is highly nonlinear in ultimate strength stage. It is important to investigate the force transfer mechanism of multi-hole perfobond connectors for determining the relationship between single-hole perfobond connection and multi-hole perfobond connectors. In this paper, two groups of push-out tests were conducted to study the behavior of multi-hole perfobond shear connectors. Combined with a simplified

mechanical model, the internal force transfer mechanism of multi-hole perfobond connection is studied extensively and the effectiveness of the multi-hole perfobond connector is also summarized.

2. Experimental study

Traditionally, the shear resistance of the shear connectors can be obtained by a small-scale push-out test. There are standard procedures for push-out tests for shear connectors in

Table1 Geometrical characteristics of specimens

Designation	Rebar diameter mm	Concrete strength (MPa)	Rib thickness (mm)	Hole diameter (mm)	Number of hole	Number of specimens
P24S	24	50	20	60	1	3
P24M	24	50	20	60	6	4

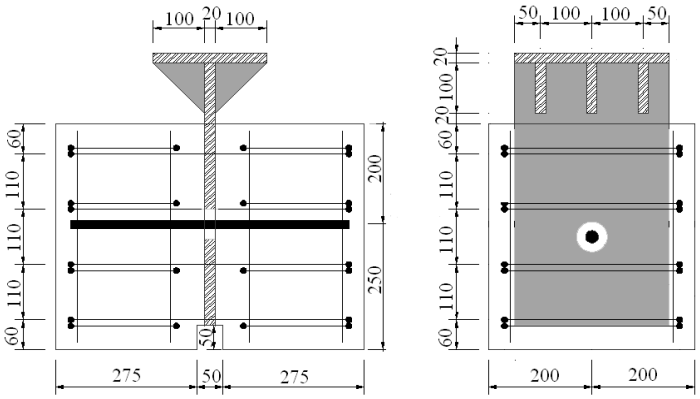

(a) P24S

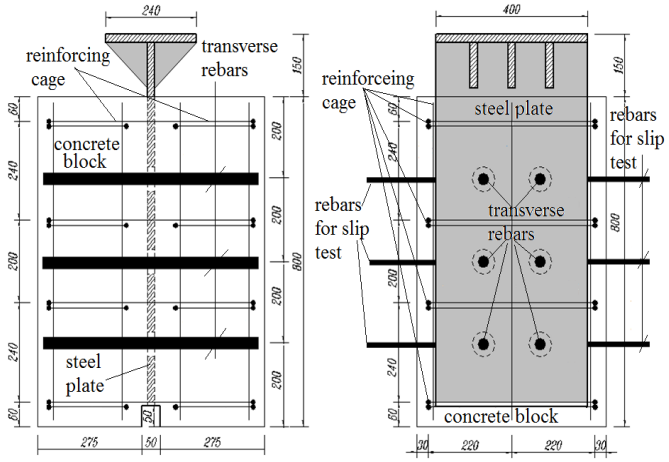

(b) P24M

Fig. 2 Dimensions of push-out test specimen

steel-concrete composite girder in Eurocode 4 and other design specifications. In addition to standard push-out test, different test methods have been proposed by researchers for different applications and details (e.g., Cho *et al.* 2012, Su *et al.* 2014). Failure modes of the perfobond rib connectors in these tests also differ from each other because of the test set up. For steel-concrete hybrid joints, the thickness of perforate plates is typically greater than 20 mm and the height of perforate plates is at least 200 mm. In some cases, perfobond shear connectors are formed by drilling holes on steel structural members.

In this study, the testing program was focused on understanding the relationship between single and multi-hole connector shear capacity. The data from the test was used for mechanistic model validation. Test specimens were divided into two different groups, namely the single and multi-hole perfobond cases. A total of seven push-out tests were conducted with some repetition for each case to ensure the accuracy of the data. The test matrix was presented in Table 1.

All of the test specimens were designed using the same concrete strength, rebar diameter, rib thickness and hole diameter, while the number of connectors are different. Table 1 summarizes the specimen configuration. According to Eurocode 4 (2005), at least three identical specimens are needed for load capacity evaluation in each group. The dimension of the specimens was shown in Fig. 2.

The perfobond connections were fabricated using 20 mm thick steel plates with Q345 steel material (a typical Chinese construction steel type, with a nominal yield stress of 345 MPa, GB50017-2003). The transverse reinforcement bars were 24 mm corrugated bars with a nominal yield stress of 335 MPa. The ratio of stirrup disposition is 0.6%.

Using a 5000 kN capacity hydraulic test machine, a monotonic loading protocol was applied to the specimens in displacement control at a speed of 4 mm/min. Fig. 3 showed the test set up and part of the instrumentation including LVDTs (Linear Variable Differential Transducers) to measure the relative longitudinal steel plate-concrete slip. The displacement gauges were installed to obtain the slip at multiple perfobond locations as shown in Fig. 4. In order to evaluate the loads within each hole of perfobond connector, strain gauges were attached to the reinforcement bars.

Fig. 3 Test setup

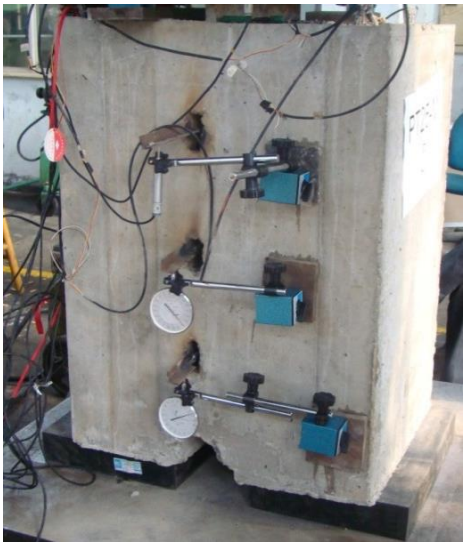

Fig. 4 Relative slips measurement

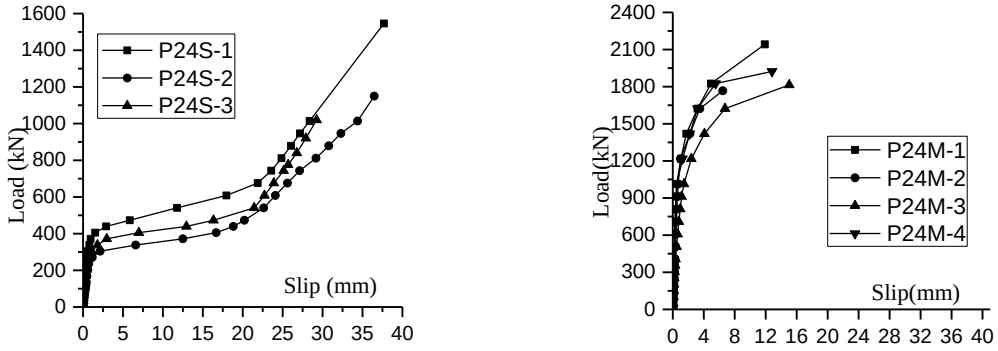

Fig. 5 load-slip curve

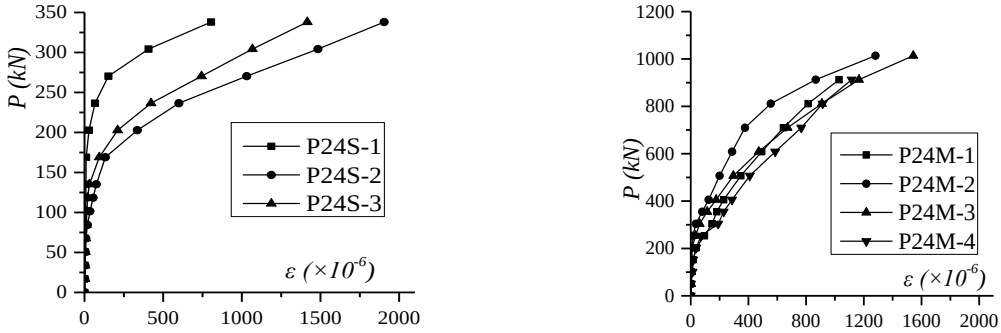

Fig. 6 load-strain curve of reinforcement bar

3. Experimental results

3.1 load-slip curves

The load-slip curves for the specimens tested were summarized in Fig. 5. The repetitions within each group yielded very similar load-slip curves. The slippage value was calculated as the average of the measurements on two sides for group P24S and the slip is the average of the measurements on three rows for group P24M. It is quite obvious that the single-hole perfobond connection exhibit significantly more ductility than multi-hole perfobond connections.

For single-hole condition, the load-slip curve can be divided into 3 stages, in the first stage, perfobond shear connector can be considered as linear elastic until the elastic bearing capacity is reached. Then a clearly defined yielding plateau with very large deformation was observed. Finally, the specimen exhibits strengthen hardening behavior till ultimate bearing capacity is reached. For multi-hole perfobond cases, the ductility of the connection is greatly reduced resulting in only two stages in load-slip curve. The ultimate load is attained at small deformation values accompanied by failure of the connection

During the tests, transversal reinforcement bars through the holes play an important role in limiting crack width and increasing ductility of the connection. Reinforcement bars also increase the shear capacities significantly. Before cracks occur in concrete block, the measured strains in reinforcement are very small (Fig. 6).

With cracks growing and slip increasing, the strains of reinforcement bar increase rapidly. It

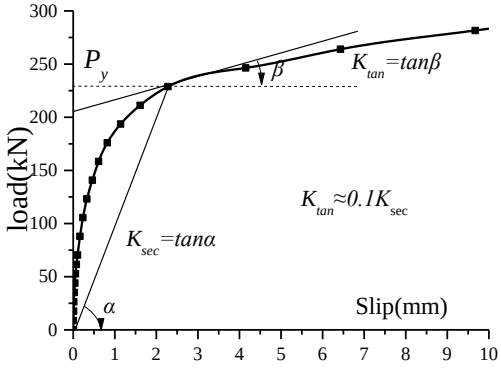

Fig. 7 characteristic parameters in load-slip curve

means that shear resistant of connectors is mainly dependent on the reinforcement at this moment. Reinforcement will close to yielding as loading increase to ultimate bearing capacity.

3.2 Characteristic parameters

In order to characterize the measured load-slip relationship from the tests, an idealized load-slip curve shown in Fig. 7 was used in this study to represent the measured responses. The parameters used in the curve include characteristic resistance (P_{Rk}), design resistance (P_{Rd}), ultimate resistance (P_u) and shear stiffness (K_s).

According to Eurocode 4, ultimate resistance P_u is equal to the maximum applied load divided by the number of connectors. Characteristic resistance P_{Rk} should be calculated considering 90% of the minimum ultimate resistance in this group, when this standard deviation is less than 10%. Design resistance P_{Rd} can be determined by the follow formulation

$$P_{Rd}=(f_u/f_{ut})(P_{Rk}/1.25)\leqslant P_{Rk}/1.25 \quad (1)$$

In Eq. (1), f_u is the ultimate strength of connection in design code, and f_{ut} is the ultimate strength of connection in practice.

Slip capacity should be taken as the largest value measured at P_{Rk}. Characteristic slip δ_{uk} should be taken as 90% of the slip capacity. Design slip δ_{Rd} should be taken as the value measured at the design resistance P_{Rd}. The load P_{Rk} is the critical point of elastic slip. When $P>P_{Rk}$, all of the slip is considered as plastic. Plastic deformation is important for multi-hole shear connector to transmit force between concrete and steel member.

In group P24S, large slip were measured before load increase to ultimate resistance. The ultimate resistance should not be used to calculate characteristic resistance, because shear resistance will be overestimated and deformation capacity will be eliminated. Yield resistance (P_y) was proposed to be a substitute for ultimate resistance in this research. Fig. 7 shows how to determine yield resistance in load-slip curve. Yield resistance can be determined in a special point, in where tangent slope is equal 10% of secant slope.

Shear stiffness is tangent slope of load-slip curve and it varies with load increasing. In practice, the ratio of design resistance to design slip can be as shear stiffness for steel-concrete structure designing. Ductility coefficient D_c is an important index to describe the ductility of shear connector, which is the ratio of the total slip at maximum load to the design slip. Table 2

Table 2 Test results

Designation		P_u kN	P_y kN	P_{Rk} kN	P_{Rd} kN	δ_u mm	δ_{Rd} mm	K_s	D_c
PT24S	1	1546	405.6	314.3	251.5	37.7	0.6	419.2	62.8
	2	1150.2	304.2			36.5	0.617	407.6	59.2
	3	1020	338			29.3	0.619	406.3	47.3
PT24M	1	357.0	236.6	186.3	149.1	11.9	0.491	303.7	24.2
	2	294.5	219.7			6.4	0.613	243.2	10.4
	3	302.4	169			15.0	0.68	219.3	22.1
	4	320.5	202.8			12.8	0.529	281.9	24.2

summarizes the characteristic parameters for different connections tested in this study.

It can be concluded that all specimens exhibited a slip capacity larger than 6 mm and meet the need of ductility in Eurocode 4. The ductility of multi-hole bond connection is significantly less than that of the single bond case. In addition, the average design resistance of a single bond in PT24M is only 59% of the design resistance of PT24S. It will be very non-conservative to calculate the design resistance of a multi-hole perfobond shear connector by multiplying the design resistance of single-hole perfobond shear connector by the number of connector. An effective reduction factor should be taking into account. This factor will be derived through a simplified mechanistic model later in this paper.

It should be pointed out that P24M have six holes with the arrangement of 3(rows)×2(lines) and line spacing will affect the total shear capacity of the connector. Generally, with lines spacing decreasing, shear resistance of multi-line perfobond ribs is decreasing. When the lines spacing is big enough, shear resistance of multi-line perfobond ribs connector tend to be constant.

3.3 Comparison of the failure modes

When perfobond shear connectors are placed in multi-hole row or multi-hole line in steel-concrete hybrid structure, every single connector is in different stress field which is changed continuously for transmitting load. Normally, since elastic deformation will occur in steel plate and concrete member, the slip of shear connector between concrete and steel member is different along the direction of shear force, and shear force would not be distributed to every connector evenly. Bearing more shear force, the connectors will lose shear resistance early, then, shear force redistribution will occur among shear connectors, and shear connector will quit work one by one with the load increasing.

The failure modes of all specimens in both groups were determined with the failure of the concrete block as it gets progressively cracked and is never conditioned by the connector failure. On the side surface of concrete block which is perpendicular to steel plate, the initial crack appeared beneath the shear rib before the ultimate load was applied, as shown in Fig. 8 and Fig. 9. The initial crack progressed along the block to the top as the load increased, and the shear resistance of the push-out specimens decreased after the cut-through crack formed on the outer surface.

In order to check the failure mode of the perfobond rib, the deformation of the rib hole and of the transverse rebar, the concrete slab was opened. It was shows that the deformation of the steel


(a) Crack in concrete


(b) Deformation of hole


(c) Deformation of transverse rebar

Fig. 8 Failure modes of specimens P24S


(a) Crack in concrete


(b) Deformation of hole


(c) Deformation of transverse rebar

Fig. 9 Failure modes of specimens P24M

rib and failure of the weld did not occur. Fig. 8 and Fig. 9 show that the deformation of the rib hole and the transverse rebar. Transverse rebar bear large shear force and bending moment for providing shear resisting in connector.

In specimens of P24M, under shear and tension stress acting, the transverse rebar located in lower row are broken, while larger deformation occurs in middle row and small deformation occurs in upper row. After the crack appears on lower of concrete block, high tensile strain are transmitted to the lower positioned reinforcement bar that crosses the main crack, when failure occurs with a more dispersed cracking along the block's height, the upper positioned reinforcement tends to be more effective and tensile stresses are higher in this zone.

4. Simplified mechanistic modeling of multi-hole perfobond joint

4.1 Joint force equilibrium and iterative solution scheme

Although a generalized 3D nonlinear finite element model can be used to simulate the behavior of perfobond joint, it is too complicated and inefficient for practical design applications. In this study, a simplified mechanistic model of multi-hole perfobond shear connector was proposed to predict the load distribution and load capacity in multi-hole perfobond shear connector. It is expected that this simplified tool can be used in design applications involving this type of joints.

Shear force distribution in multi-hole perfobond shear connectors is similar to that of a multi-hole bolt joint. The loading diagram of multi-hole perfobond shear connector over uniform

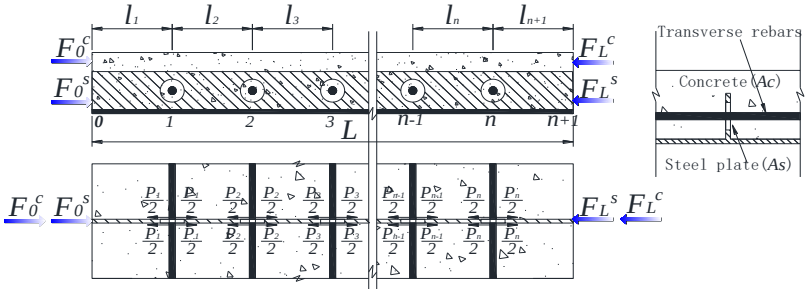

Fig. 10 Load condition in multi-hole perfobond shear connectors

axial load can be idealized as shown in Fig. 10.

Where F_0^s is the axial force at the loading end of steel plate, and F_L^s is the axial force at the bounding end of steel plate. F_0^c is the axial force at the loading side of concrete member, and F_L^c is the axial force at the cross section of concrete member

For ultimate strength calculation, neglecting the friction and adhesion between steel and concrete, the total shear force V carried by all shear connector meet the equilibrium equation

$$F_0^s - F_L^s = V = F_L^c - F_0^c \tag{2}$$

For any single connector, shear force carried by it, P_i, can be calculated by using the following formulation

$$P_i = f(S_i) = f(d_i^s - d_i^c) \qquad i = 1,2,3\ldots\ldots n \tag{3}$$

Where, d_i^s is the deformation of steel plate at the position of connector, d_i^c is the deformation of concrete at the position of connector. $f(x)$ is a function between shear force P_i and relative slip S_i.

Thus, relative slip S_i is given as

$$S_i = d_i^s - d_i^c \tag{4}$$

The total shear force equal the sum of shear force of every single connector.

$$V = \sum_{i=1}^{n} P_i \tag{5}$$

Substituting Eq. (5) to Eq. (2)

$$F_0^s - F_L^s = \sum_{i=1}^{n} P_i = F_L^c - F_0^c \tag{6}$$

Taking every shear connector as a separating point, the connection can be divided into n+1 isolation units. Load mode of any isolation units under longitudinal force is shown in Fig. 11.

For steel plate, elastic compression deformation depends on the compression load, cross section area, length of the plate, and the elastic module. Assuming the load is uniformly distributed throughout steel cross section, the equation for the elastic compression deformation of steel plate can be expressed as

$$d_i^s - d_{i+1}^s = \frac{F_0^s - \sum_{j=1}^{i} P_j}{E_s \cdot A_s^i} l_i \quad (i = 0,1,2\cdots n) \tag{7}$$

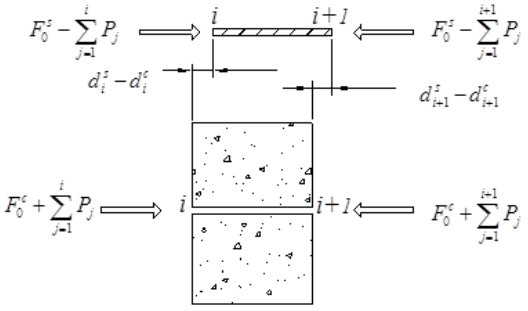

Fig. 11 Load mode of isolation units

Where, d_0^s is the displacement of steel plate at the beginning of section, d_{n+1}^s is the displacement of steel plate at the end of section.

Similarly, the equation for the elastic compression deformation of concrete member can be expressed as

$$d_i^c - d_{i+1}^c = \frac{F_0^c + \sum_{j=1}^{i} P_j}{E_c \cdot A_c^i} l_i \quad (i = 0,1,2 \cdots n) \tag{8}$$

Where, d_0^c is the deformation of concrete member at the beginning of section, d_{n+1}^c is the deformation of concrete member at the end of section.

Generally, the location of steel-concrete hybrid member can be determined at first, and a variables among d_0^s, d_{n+1}^s, d_0^c, d_{n+1}^c should be a known quantity, so given that d_{n+1}^c is known.

Based on Eq. (6) to Eq. (8), $3n+3$ equations can be listed. Given the force boundary conditions, thus F_0^s, F_L^s, F_L^c and F_0^c are become known number, while d_i^c (i=0,1,2…n), d_i^s (i=0,1,2…n,n+1) and P_i(i=0,1,2…n) are unknown quantities. There are $3n+3$ unknown quantities in $3n+3$ simultaneous equations, so the equations could be solved.

When subtract Eq. (8) from Eq. (7)

$$\begin{aligned} & d_i^s - d_i^c - (d_{i+1}^s - d_{i+1}^c) \\ & = \frac{F_0^s - \sum_{j=1}^{i} P_j}{E_s \cdot A_s^i} l_i - \frac{F_0^c + \sum_{j=1}^{i} P_j}{E_c \cdot A_c^i} l_i \quad (i = 0,1,2 \cdots n) \end{aligned} \tag{9}$$

Substituting Eq. (3) and Eq. (4) to Eq. (9)

$$\begin{aligned} & S_i - S_{i+1} + (\frac{1}{E_s \cdot A_s^i} + \frac{1}{E_c \cdot A_c^i}) \cdot l_i \cdot \sum_{j=1}^{i} f(S_j) \\ & = (\frac{F_0^s \cdot l_i}{E_s \cdot A_s^i} - \frac{F_0^c \cdot l_i}{E_c \cdot A_c^i}) \quad (i = 0,1,2 \cdots n) \end{aligned} \tag{10}$$

Substituting Eq. (3) to Eq. (6)

$$\sum_{i=1}^{n} f(S_i) = F_0^s - F_0^c \tag{11}$$

Eq. (10) and Eq. (11) are the compatibility equation of relationship between load and slip in multi-hole perfobond shear connectors. It is a set of nonlinear equation with unknown variable, S_i, which can be solved by iterative method.

4.2 Iterative solution scheme

Using Newton-Raphson iterative methods, Eq. (10) and Eq. (11) were solved. Alternatively, Eq. (10) and Eq. (11) can be expressed as in matrix form as

$$[K(S)]\{S\}=\{F\} \tag{12}$$

Where, $[K(S)]$ is generalized stiffness matrix, $\{S\}$ is generalized displacement vector, and $\{F\}$ is generalized load vector.

Given an initial displacement vector S_0, if $\{S_i\}$ is the slip solved by i times iteration under n times load steps, then the control equation can be expressed as

$$\begin{aligned}\left[K_i^T\right]\{\Delta S_i\}&=\{F\}-\left\{F_i^{nr}\right\}\\ \{S_{i+1}\}&=\{S_i\}+\{\Delta S_i\}\end{aligned} \tag{13}$$

Where, $[K_i^T]$ is the tangent stiffness matrix in i times iteration, $\{F_i^{nr}\}$ is the restoring force calculated by substituting $\{S_i\}$. After slips S_i are determined, shear force P_i suffering by every connector can be calculated by Eq. (3).

Numerical convergence problem always occurs in Finite Element (FE) analysis because of element distortion and nonlinear effect as the connection deforms into the second stage (defined in section 2.3). The iterative analytical solution is significantly simpler than FE method and can easily be implemented using Excel or Matlab. This makes it suitable for design calculations of these types of connection. In this study, the simplified analytical model result and push-out test result are compared and shown in Fig. 12.

It can be seen that the result from simplified calculation agrees well with the push-out test result. Based on the comparison of iterative calculation to test, it is clear that this mechanistic model can be used to predict shear resistance of shear connector. The simplified model is also accurate enough for engineering application.

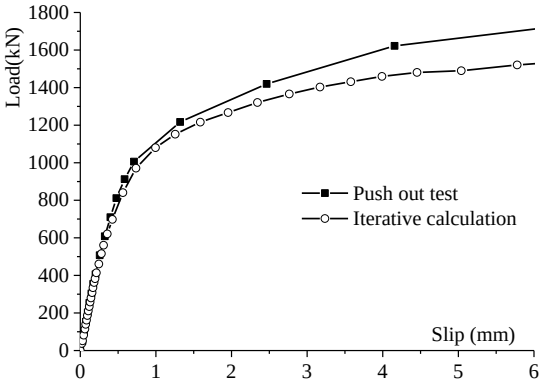

Fig. 12 Result from push-out test and iterative calculation

4.3 Mechanistic model simplification

Generally, perfobond shear connectors are always arranged in same spacing. So, in Eq. (10) A^i_c, A^i_s and l^i are all constant value. Given $A^i_c=A_c$, $A^i_s=A_s$ and $l^i=l$, Eq. (10) can be simplified as

$$\begin{aligned} & S_i - S_{i+1} + (\frac{l}{E_s \cdot A_s} + \frac{l}{E_c \cdot A_c}) \sum_{j=1}^{i} f(S_i) \\ & = \frac{F_0^s \cdot l}{E_s \cdot A_s} - \frac{F_0^c \cdot l}{E_c \cdot A_c} \end{aligned} \tag{14}$$

Given $\frac{l}{E_s \cdot A_s} + \frac{l}{E_c \cdot A_c} = \alpha$, $\frac{F_0^s \cdot l}{E_s \cdot A_s} - \frac{F_0^c \cdot l}{E_c \cdot A_c} = \beta$, Eq. (14) can be expressed as

$$S_{i+1} = S_i + \alpha \sum_{j=1}^{i} f(S_j) - \beta \tag{15}$$

The Load-slip relationship of shear connector can be expressed as

$$P=K(S) \cdot S \tag{16}$$

Where, $K(S)$ is shear stiffness function, which is effected by some design parameters (e.g., hole diameter, steel bar diameter, steel plate thickness and concrete strength, etc.) and varied with relative slip.

Using a bilinear fitting mode, the load-slip relationship of shear connector can be described in Fig. 13. The gradient of the straight line joining the points (0,0) and (P_{Rd}, S_{Rd}) can be defined as the shear stiffness, K_s, for structure design in the serviceability limit states. While, the gradient of the straight line joining the points (P_{Rd}, δ_{Rd}) and (P_u, δ_u) can be defined as the shear stiffness, K_u, for structure design in the ultimate limit states.

Thus, Eq. (16) can be expressed as a bilinear-spring model

$$P = \begin{cases} K_s \cdot S & S \le \delta_{Rd} \\ P_{Rd} + K_u \cdot (S - \delta_{Rd}) & S > \delta_{Rd} \end{cases} \tag{17}$$

For multi-hole perfobond shear connector, if all connector worked under the serviceability limit states, Eq. (3) would be expressed as

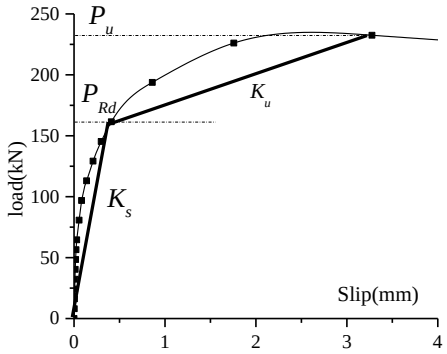

Fig. 13 Bilinear shear stiffness of perfobond shear connector

$$P_i = f(S_i) = K_s \cdot S_i \tag{18}$$

Substituting Eq. (18) to Eq. (15), Eq. (15) would be developed as

$$\begin{cases} S_1 = S_0 - \beta \\ S_2 = S_1 + \alpha K_S \cdot S_1 - \beta = (1+\alpha K_S)S_0 - (2+\alpha K_S)\beta \\ S_3 = S_2 + \alpha K_S(S_1 + S_2) - \beta = (\alpha^2 K_S{}^2 + 3\alpha K_S + 1)S_0 - (\alpha^2 K_S{}^2 + 5\alpha K_S + 3)\beta \\ S_4 = S_3 + \alpha K_S(S_1 + S_2 + S_3) - \beta \\ \quad = (\alpha^3 K_S{}^3 + 5\alpha^2 K_S{}^2 + 6\alpha K_S + 1)S_0 - (\alpha^3 K_S{}^3 + 7\alpha^2 K_S{}^2 + 11\alpha K_S + 4)\beta \\ S_n = S_{n-1} + \alpha K_S \sum_{i=1}^{n-1} S_i - \beta \end{cases} \tag{19}$$

Given α, β and K_s, based on Eq. (19), S_i could be expressed as an algebraic expression about S_0. Then, substituting all algebraic expressions to Eq. (11), S_0 is solved. When S_0 is determined, S_i can be solved by Eq. (19) and P_i would be obtained by Eq. (18). The internal shear force distribution of multi-hole perfobond would be solved in high efficiency by a simple computer program based on Eq. (19). Shear stiffness of the connector K_s is effected by some design parameters (e.g., hole diameter, steel bar diameter, steel plate thickness and concrete strength, etc.). Currently, no united formula can be used to calculate K_s and push-out tests are needed for each sized connector. When design resistance P_{Rd} and design slip of single-hole perfobond-rib shear connector were determined by push-out test, shear stiffness of the connector K_s in elastic state can be defined as following equation:

$$K_s = P_{Rd}/\delta_{Rd}$$

In order to analysis the behavior of multi-hole perfobond shear connector in the ultimate limit states, shear stiffness K_s should be revised according to relative slip, after solving Eq. (11) iteratively and S_i are determined.

5. Multi-hole perfobond shear behavior and efficiency coefficient

5.1 shear force distribution

In Fig. 14, the test-measured percentage of the shear force acting on shear connector in every rows of P24M (relative to the total shear load) was compared with the simplified calculation.

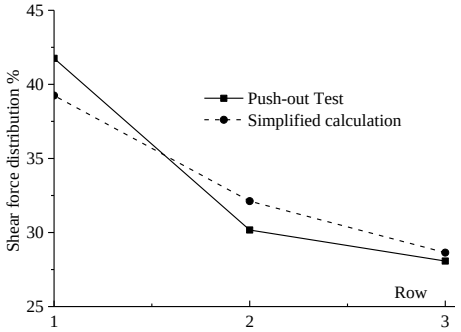

Fig. 14 Shear force distribution in every rows

As an indeterminate structural system, shear force distribution among shear connectors in multi-hole perfobond connection depends on the relative slip at each connector location. The percentage shown in Fig. 14 was based on the data at the ultimate strength loading. The simplified method captures the load sharing characteristics of the perfobond connection very well, this also signifies the level of accuracy for the proposed model from a mechanistic standpoint.

For multi-hole perfobond connection design, it is beneficial to look into how shear transfer mechanism at each row of connectors change with different connection design. Using the mechanistic model developed in this study, the trend in the change of shear force sharing with respect to varying multi-hole perfobond joint configuration was studied in detail as presented in this section.

Given $F_0^s=Q$, $F_0^c=0$, Eq. (20) can be obtained through rearrangement of the terms based on formulate Eq. (19).

$$(n-1)\frac{K_s l}{E_s A_s}Q = F_1 - F_n + \left(1+\frac{E_s A_s}{E_c A_c}\right)\frac{K_s l}{E_s A_s}\sum_{i=1}^{n-1}(n-i)F_i \tag{20}$$

Defining the stiffness ratio of steel to concrete member (STC) is λ and stiffness ratio of perfobond shear connector to steel member (PTS) is ξ.

$$\frac{K_s l}{E_s A_s} = \xi \qquad \frac{E_c A_c}{E_s A_s} = \lambda$$

Eq. (20) can be expressed as

$$(n-1)\xi Q = F_1 - F_n - (1+\lambda)\xi\sum_{i=1}^{n-1}(n-i)\cdot f\left(F_1,\lambda,\xi,Q\right)_i \tag{21}$$

From Eq. (21), it can be concluded that shear forces distribution were determined by some character parameters including stiffness ratio of STC λ, stiffness ratio of PTS ξ, and number of row n. Note these ratios are defined to be dimensionless and can be easily obtained from any perfobond connection design.

In elastic state, slippage of every connector less than design slip δ_{Rd}, and the relationships of shear force distribution percentage and character parameters were investigated by using the proposed analytical model. The results are shown in Fig. 15. In Figs. 15(a)-(b), row number of multi-hole perfobond shear connectors equal 10.

Fig. 15 shows the trend of shear forces distribution between each row in multi-hole perfobond shear connector is changing with joint design. Shear force distribution curve is close to catenary. High shear force will act on the connectors in the end rows of multi-hole perfobond shear connector, while, low shear force will act on the connectors in the middle rows. Different character parameters have different effect on shear distribution. For stiffness ratio of STC λ, with λ increasing the location of maximum shear changed from row 1 to row 10, and when λ=1.0, bilateral symmetry shear force distribution occurs in shear connectors. Increasing the stiffness ratio of PTS ξ, shear force distribution is more non-uniform. When number of row n is increased to some value, shear connector bear fewer shear force in middle section compared it in end section, and with n increasing, shear force distribution is more non-uniform.

Generally, shear resistance of perfobond ribs connector can be increased by increasing row number. However, with the row number increasing, the connectors have lower efficiency of shear resistance. With different row number and different stiffness ratio ξ, total shear force of perfobond

ribs connector in elastic state were shown in Fig. 16.

It can be concluded that the stiffness of shear connector is higher and the efficiency of shear transmission is lower, which is means increasing the stiffness ratio ξ. the conclusions are in line with the results obtained by Kim *et al.* (2014, 2015).

5.2 single connector efficiency coefficient

Based on the shear force distribution in multi-hole perfobond shear connector, the behavior of multi-hole perfobond shear connector can be divided into three phases including elastic stage,

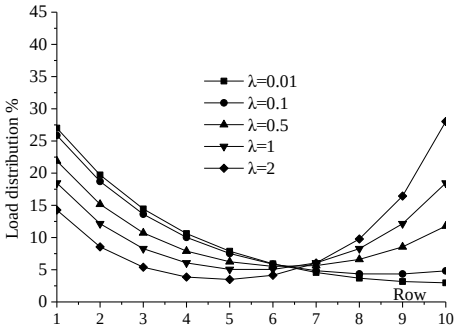

(a) Shear force distribution with different λ (ξ=0.1)

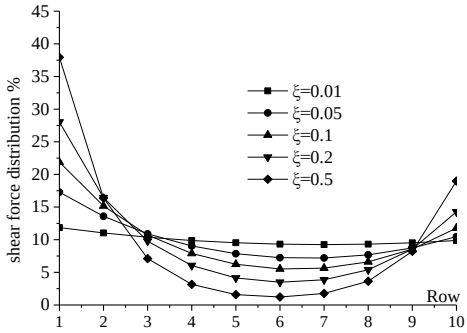

(b) Shear force distribution with different ξ (λ=0.5)

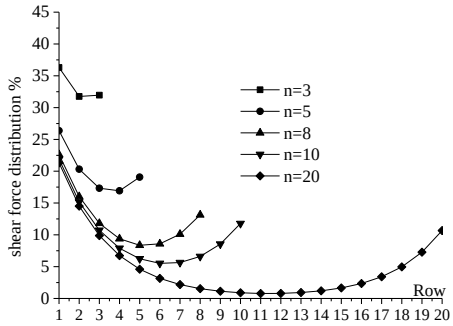

(c) Number of rows n (ξ=0.1, λ=0.5)

Fig. 15 shear force distribution in different design parameter

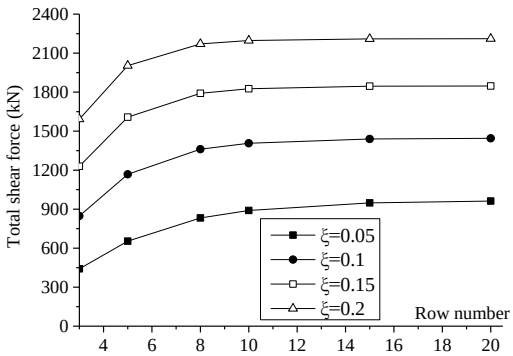

Fig. 16 Total shear force of multi-hole perfobond ribs connector (λ=0.5)

single end plastic stage, and both ends plastic stage. In elastic stage, the slip of any connectors is less than the design slip δ_{Rd}. In single end plastic stage, slips of partial connectors in single end beyond the design slip δ_{Rd}. In both ends plastic stage, slips of partial connectors in both ends beyond the design slip δ_{Rd}. Therefore, three limit states were proposed depends on the three stages. In single edge yielding limit state, the slip of one connector equals the design slip δ_{Rd} on the one edge of multi-hole perfobond shear connector. With loading increasing, the slip of connector on the other edge increase to the design slip δ_{Rd} in both edges yielding limit state. In ultimate limit states, the slips of partial connectors beyond the characteristic slip δ_{uk} and multi-hole perfobond shear connector bearing maximum shear force.

Considering the shear force distribution in multi-hole perfobond shear connector, we define efficiency coefficient of shear resistance η as: $\eta=P_{md}/(n.P_{Rd})$.

Where, P_{md} is design resistance of multi-hole perfobond shear connection, P_{Rd} is design resistance of single perfobond shear connector. Thus in a simplified design of multi-hole perfobond connection, the total design load can be calculated by multiplying the number of single connector by this efficiency coefficient and the total number of connectors. In a multi-hole perfobond connection design, there are 3 parameters that are crucial to the performance of the global joint behavior, namely the stiffness ratio of PTS ξ, the stiffness ratio of STC λ, and row number. In this section, the interaction of these parameters to the calculation of the connection strength is studied in detail with empirical formulas proposed for the design of these joints.

In single edge yielding limit state, all connectors work in elastic stage and the effective coefficients are showed in Fig. 17. Increasing the stiffness ratio ξ, effective coefficient is decreased greatly following a power function. Effective coefficient increases near linearly with λ increasing when λ less than 1.0, while effective coefficient decreases with λ increasing when λ beyond 1.0. As the number of rows n is increasing, effective coefficient decreases.

Based on the effective coefficient result from different character parameters, a relation formulation were obtained by function fitting, which can be expressed as

$$\eta=\begin{cases}\left(0.1173\lambda+0.1591\right)\ \xi^{(0.087\lambda-0.3565)} & (\lambda\le 1)\\ \left(0.2638\lambda^{-0.51}\right)\ \xi^{(0.0056\lambda^2-0.037\lambda-0.2524)} & (\lambda\ge 1)\end{cases}(N=10) \tag{22}$$

Generally, λ is always less than 1.0, so Eq. (22) would be developed as Eq. (23) considering the effect of row number.

$$\eta=\left(0.146n^{-1.114}\cdot\lambda+2.096n^{-1.112}\right)\ \xi^{\left[(0.1308-0.0042n)\lambda+0.0011n^2-0.038n-0.0756\right]}\qquad(\lambda\le 1) \tag{23}$$

Taking into account the relationship between effective coefficient and different character parameters, the stiffness ratio of PTS ξ should less than 0.2 and stiffness ratio of STC λ should be great than 0.1, in order to provide high bearing efficiency.

It was showed in Fig. 17, when row number is greater than 5, effective coefficient may be less than 0.5 in single edge yielding limit state. Actually, multi-hole perfobond shear connector can bear more loads, and single edge yielding limit state should not be defined as the design limit state.

Obviously, yielding mode will change with λ as it is showed in Fig. 17. When λ=1.0, connectors yield in both edge at the same time and plastic zones extend simultaneously with load increasing. Decreasing the value of λ, connectors yield in single edge firstly and different plastic zones range exist in two edges with load increasing. Decreasing λ to some value, connectors yield in single edge and single plastic zone is kept with load increasing, so both edges yielding limit state will not

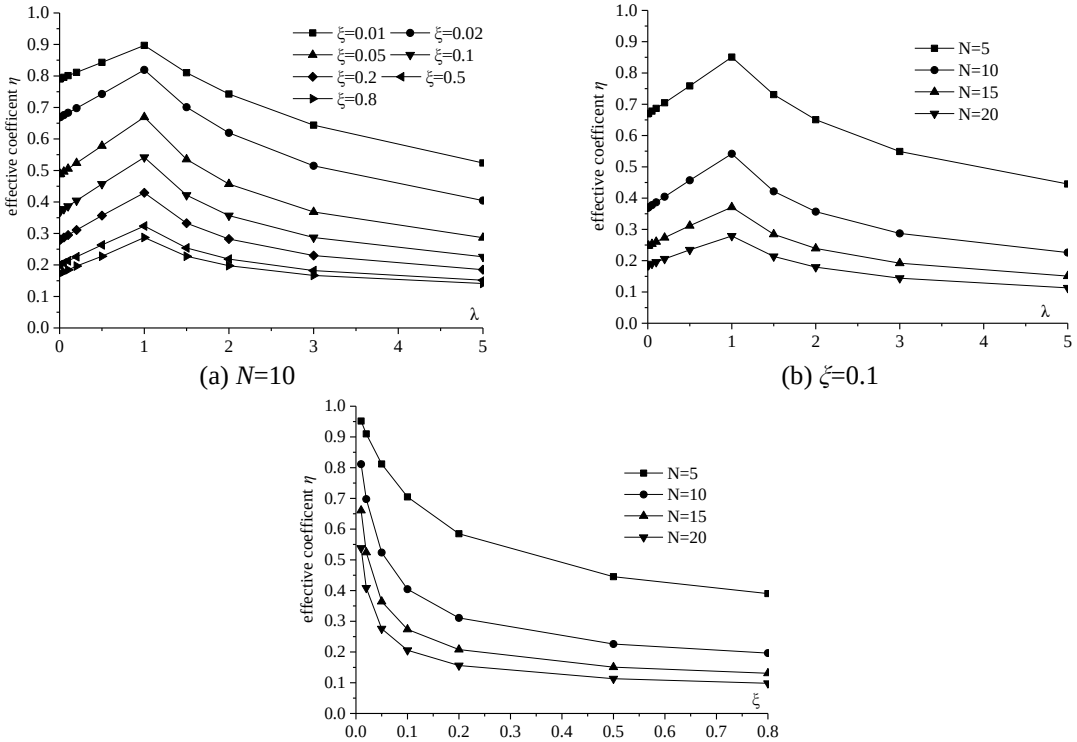

(a) N=10 (b) ξ=0.1

(c) λ=0.2

Fig. 17 effective coefficient in single edge yielding limit state

occur. For practical application in design of steel-concrete structure, maximum average slippage or yield proportion should be used to define the design limit state of multi-hole perfobond shear connector. At the view of deformation, the average value of slippage in every connector is equal to the maximum average slippage in design limit state. While, at the view of bearing capacity, the ratio of the number of yield connectors to the number of total connectors is equal to the yield proportion in design limit state. The value of maximum average slippage or yield proportion need be investigated by the series research in the future.

6. Conclusions

A comprehensive study on the multi-hole perfobond shear connector in steel-concrete hybrid structure has been conducted and the following conclusions can be made based on the push-out test and shear force transfer mechanism analysis.

• Push-out test results show that design resistance of a multi-hole perfobond shear connector should not be obtained by multiplying the design resistance of single-hole perfobond shear connector by the number of connector simply. An efficiency coefficient should be taking into account in different limit state.

• For multi-hole perfobond shear connector, shear force distribution curve is near catenary. Shear forces distribution were determined by some character parameters including stiffness ratio

of STC λ, stiffness ratio of PTS ξ, and number of row n.

• The location of maximum shear changed with λ increasing, and when λ=1.0, bilateral symmetry shear force distribution occurs in shear connectors. Increasing ξ or n, shear force distribution is more non-uniform. Taking into account the relationship between effective coefficient and different character parameters, the stiffness ratio of PTS ξ should less than 0.2 and stiffness ratio of STC λ should be great than 0.1, in order to provide high bearing efficiency.

• The behavior of multi-hole perfobond shear connector can be divided into three phases including elastic stage, single edge plastic stage, and both edges plastic stage. Both edge yielding and single edge yielding are mainly two kinds of ultimate limit states, which is changed by different λ.

• Single edge yielding limit state should not be looked as the design limit state of multi-hole perfobond shear connector. Maximum average slippage or yield proportion should be used for design, which need be investigated by the series research in the future.

Acknowledgments

The research described in this paper was financially supported by National Science Founding of China (NSFC) Project 50808150 and 51308467. Thanks are also owed to the Structures Engineering Laboratory of Southwest Jiaotong University, where the tests were conducted.

References

Ahn, J.H., Lee, C.G., Won, J.H. and Kim, H.Y. (2010), "Shear resistance of the perfobond-rib shear connector depending on *concrete* strength and rib arrangement", *J. Constr. Steel Res.*, **66**(10), 1295-1307.

Cândido-Martins, J.P.S., Costa-Neves, L.F. and Vellasco, P.C.G.S. (2010), "Experimental evaluation of the structural response of perfobond shear connectors", *Eng. Struct.*, **32**(8), 1976-85.

Chung, C.H. and Lee, H.S. (2005), "Evaluation of shear strength of the type perfobond rib shear connectors", *J. Korea Soc. Civil Eng.*, KSCE, **25**(5A), 879-888. (In Korean)

Cho, J.R., Park, S.Y., Cho, K., Kim, S.T. and Kim, B.S. (2012), "Pull-out test and discrete spring model of fiber reinforced polymer perfobond rib shear connector", *Can. J. Civil Eng.*, **39**(12), 1311-1320.

Costa-Neves, L.F., Figueiredo, J.P., Vellasco, P.C.G.S. and Vianna, J.D.C. (2013), "Perforated shear connectors on composite girders under monotonic loading: An experimental approach", *Eng. Struct.*, **56**(6), 721-737.

EUROCODE 4. EN 1994-1-1 (2005), *Design of composite steel and concrete structures Part 1.1 General rules and rules for buildings*, CEN-European Committee for Standardization, Brussels.

Hamed, A., Mehdi, D., Morteza, H.B. and Ebrahim, R. (2014), "Mechanical behavior of steel-concrete composite decks with perfobond shear connectors", *Steel Compos. Struct.*, **17**(3), 339-358.

Kim, H.Y. and Jeong, Y.J. (2006), "Experimental investigation on behavior of steel-concrete composite bridge slabs with *perfobond* ribs", *J. Constr. Steel Res.*, **62**(5), 463-471.

Kim, S.H., Choi, K.T., Park, S.J., Park, S.M. and Jung, C.Y. (2013), "Experimental shear resistance evaluation of Y-type perfobond rib shear connector", *J. Constr. Steel Res.*, **82**(3), 1-18.

Kim, S.H., Choi, J., Park, S.J., Ahn, J.H and Jung, C.Y. (2014), "Behavior of composite girder with Y-type perfobond rib shear connectors", *J. Constr. Steel Res.*, **103**(12), 275-289.

Kim, S.H., Park, S.J., Heo, W.H. and Jung, C.Y. (2015), "Shear resistance characteristic and ductility of Y-type perfobond rib shear *connector*", *Steel Compos. Struct.*, **18**(2), 497-517.

Leonhardt, F., Andra, W., Andra, H.P. and Harre, W. (1987), "New improved bonding means for composite

load-bearing structures with high fatigue strength", *Beton Stahlbetonbau*, **82**(12), 325-331. (in German)
Medberry, S.B. and Shahrooz, B.U. (2002), "Perfobond shear connector for composite construction", *Eng. J.*, **39**(1), 2-12.
Ministry of Construction of China. GB50017-2003 (2003), *Code for design of steel structures*, China Planning Press, Beijing.
Oguejiofor, E.C. and Hosain, M.U. (1997), "Numerical analysis of push-out specimens with perfobond rib connectors", *Comput. Struct.*, **62**(4), 617-624.
Rodrigues, J.P.C. and Laím, L. (2011), "Behaviour of perfobond shear connectors at high temperatures", *Eng. Struct.*, **33**(10), 2744-2753.
Su, Q.T., Wang, W., Luan, H.W. and Yang, G.T. (2014), "Experimental research on bearing mechanism of perfobond rib shear connectors", *J. Constr. Steel Res.*, **95**(2), 22-31.
Veldanda, M.R. and Hosain, M.U. (1992), "Behaviour of perfobond rib shear connector: push-out tests", *Can. J. Civil Eng.*, **19**(1), l-10.
Vianna, J.C., Costa-Neves, L.F., Vellasco, P.C.G.S. and Andrade, S.A.L.D. (2009), "Experimental assessment of Perfobond and T-Perfobond shear connectors", *J. Constr. Steel Res.*, **65**(2), 408-421.
Vianna, J.C., Andrade, S.A.L.D., Vellasco, P.C.G.S. and Costa-Neves, L.F. (2013), "Experimental study of Perfobond shear connectors in composite construction", *J. Constr. Steel Res.*, **81**(2), 62-75.
Wei, X. and Xiao, G.L. (2011), "Shear resistance of perfobond shear connectors in steel-concrete composite structure based on BP neural network", *J. Highw. Tran. Res. Develop.*, **28**(10), 60-64. (in Chinese)
Wei, X. and Xiao, L. (2013), "Mechanical behavior and failure mechanism of perfobond shear connectors in steel-concrete hybrid structure", *IABSE Symposium Report*, *IABSE*, **99**(26), 178-179.
Zellner, W. (1987), "Recent designs of composite bridges and a new type of shear connectors", *Proceedings of the IABSE/ASCE Engineering Foundation Conference on Composite Construction*, New England College, USA.

CC